On the model-dependence of the relation between minimum-bias and inelastic proton-proton cross sections

S. Ostapchenko

NTNU, Institutt for fysikk, 7491 Trondheim, Norway

D.V. Skobeltsyn Institute of Nuclear Physics, Moscow State University, 119992 Moscow, Russia

January 18, 2013

Abstract

The model-dependence of the relation between the inelastic and various minimum-bias proton-proton cross sections is analyzed, paying a special attention to the sensitivity of minimum-bias triggers to diffractive collisions. Concentrating on the trigger selections of the ATLAS experiment, the measured cross sections are compared to predictions of a number of hadronic Monte Carlo models used in the cosmic ray field. It is demonstrated that the ATLAS results are able to discriminate between different models and between certain theoretical approaches for soft multi-particle production. On the other hand, the strong model-dependence of the selection efficiency of the minimum-bias triggers prevents one from inferring high mass diffraction rate from the discussed data. Moreover, the measured cross sections prove to be insensitive to the production of low mass diffractive states in proton-proton collisions. Consequently, a reliable determination of the total inelastic cross section requires forward proton tracking by a dedicated experiment.

1 Introduction

The knowledge of the inelastic proton-proton cross section and of its repartition into the non-diffractive one and into partial cross sections for various diffractive processes is of considerable importance for understanding the dynamics of strong interactions. Additionally, it is involved into determinations of collider luminosities and into normalizations of measured particle spectra. On the other hand, a proper understanding of the energy-dependence of the inelastic and diffractive pp cross sections is of vital importance for experimental studies of high energy cosmic rays. Due to an extremely low incoming flux of such particles, their properties are inferred from measured characteristics of nuclear-electromagnetic cascades - extensive air showers induced by them in the air. In turn, the longitudinal development of air showers depends strongly on the magnitude of $\sigma_{pp}^{\rm inel}$ and on the relative rate of diffractive interactions [1].

It has been proposed recently [2] that a study of minimum-bias cross sections at the Large Hadron Collider (LHC) with various combinations of triggering detectors could be a powerful instrument for discriminating between theoretical approaches to hadronic multiple production and may allow one to infer the rate of diffraction at LHC energies. Presently, such a study in underway by the ATLAS, CMS, and ALICE Collaborations [3] and the first results for the observed minimum-bias cross sections have been reported by ATLAS [4].

The purpose of the present work is twofold. First, we investigate model-dependence of the relation between various minimum-bias cross sections and $\sigma_{pp}^{\rm inel}$, in particular, concerning the contributions of low and high mass diffraction dissociation. Secondly, we check if the ATLAS data are able to discriminate between different models of hadronic interactions, in particular, between the ones used to treat cosmic ray interactions in the atmosphere.

2 Model approaches

General inelastic hadron-hadron collisions receive large contributions from soft processes and cannot be treated within the perturbative QCD framework. This is especially so concerning the inelastic diffraction which is often described in hadronic Monte Carlo (MC) generators in a purely phenomenological way: based on empirical parametrizations for the corresponding partial cross sections and assuming a simple dM_X^2/M_X^2 distribution for the mass squared of diffractive states produced [5]. The only, though still phenomenological, approach which offers a microscopic treatment of general soft and, in particular, diffractive collisions of hadrons is provided by Gribov's Reggeon Field Theory (RFT) [6]. In the RFT framework, hadron-hadron collisions are described as multiple scattering processes, with "elementary" scattering contributions being treated as Pomeron exchanges. One usually employs separate treatments for low ($M_X^2 \lesssim 10$ GeV^2) and high mass diffractive excitations. The former can be conveniently described using the Good-Walker-like multi-channel approach [7, 8]: representing the interacting hadrons by superpositions of a number of elastic scattering eigenstates characterized by different interaction strengths and, generally, different transverse profiles. Assuming eikonal vertices for Pomeron-hadron coupling, one obtains simple expressions for partial cross sections of various low mass diffraction processes. On the other hand, high mass diffraction is related to the so-called enhanced diagrams which involve Pomeron-Pomeron interactions [9], with the triple-Pomeron coupling as the key parameter of the scheme. Importantly, at higher energies enhanced graphs of more and more complicated topologies contribute to elastic scattering amplitude and to partial cross sections of various, notably diffractive, final states. Hence, meaningful results can only be obtained after a full resummation of all significant enhanced contributions, to all orders with respect to the triple-Pomeron coupling [10].

In this work, we analyze model-dependence of the relation between $\sigma_{pp}^{\rm inel}$ and various minimum-bias proton-proton cross sections, paying a special attention to the sensitivity of minimum-bias triggers to diffractive collisions. We concentrate on the trigger selections of the ATLAS experiment [4] and employ in this study hadronic MC generators used in the cosmic ray field. In particular, we use the most recent version of the QGSJET-II model (QGSJET-II-04) [11] which is the only MC generator based on the full all-order resummation of enhanced Pomeron graphs and which thus provides the theoretically most advanced treatment of the physics relevant to the present study.[1] The corresponding results will be compared to the ones of the SIBYLL model [18, 19] which describes inelastic diffraction similarly to the PYTHIA generator [5, 20]: dM_X^2/M_X^2 distribution is used for diffractive mass squared and no special treatment for low mass diffraction is employed. In addition, we use the previous version of QGSJET-II (QGSJET-II-03) [21] which was based on the resummation of "net"-like enhanced Pomeron graphs while neglecting Pomeron "loop" contributions [22]. As a consequence, there is a factor of two difference in the value of the triple-Pomeron coupling between the two model versions, which projects itself in the corresponding difference for the predicted single high mass diffraction cross section. On the other hand, the inclusion of Pomeron loops significantly enhances the rate of double high mass diffraction in QGSJET-II-04 compared to QGSJET-II-03. While both model versions employ a 2-component multi-channel approach for describing low mass diffraction, QGSJET-II-04 differs from the previous version by using different transverse profiles for Pomeron emission vertices by different elastic scattering eigenstates [11].[2] This had the consequence of a significantly larger low mass diffraction rate at very high energies in QGSJET-II-04. The three models considered differ also in their predictions for the high energy behavior of total and inelastic proton-proton cross sections, as shown in Fig. 1, which is partly related to model calibrations to the CDF [24] or E710 [25] results on $\sigma_{pp}^{\rm tot}$ at the Tevatron. A comparison of the three models' results with various accelerator data, from fixed target energies up to LHC,

[1] Alternative approaches to the resummation of enhanced Pomeron diagrams have been proposed in Refs. [12, 13, 14, 15, 16, 17].

[2] The choice of different profiles for the eigenstates was necessary to get an agreement with measured differential elastic cross section for hadron-proton collisions. On the other hand, such an agreement could be obtained using the same transverse profile for all the eigenstates but choosing a more sophisticated profile shape [13].

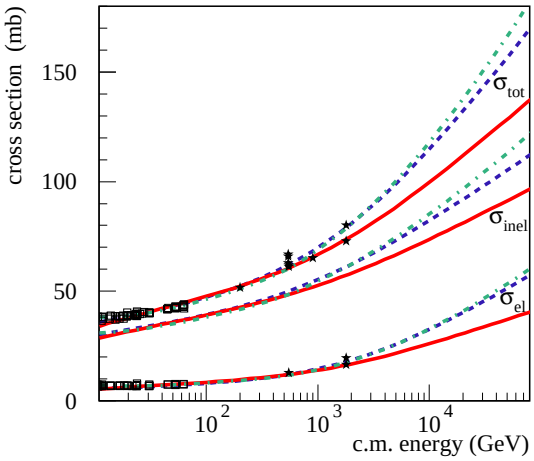

Figure **1**: Model predictions for total, elastic, and inelastic proton-proton cross sections: QGSJET-II-4 - solid, QGSJET-II-3 - dashed, and SIBYLL - dot-dashed. The compilation of data is from Ref. [23].

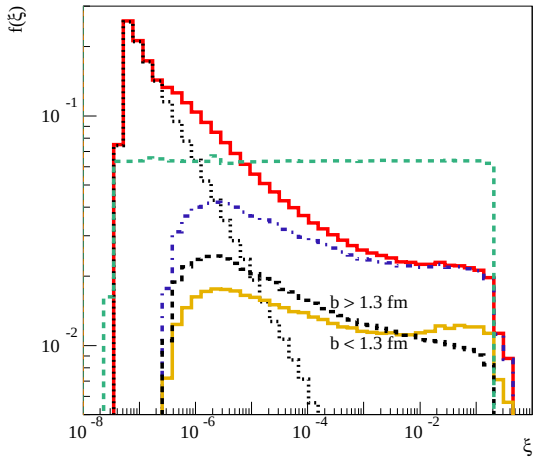

Figure **2**: $f_{\rm SD}(\xi) \equiv \frac{\xi}{\sigma_{\rm SD}} \frac{d\sigma_{\rm SD}}{d\xi}$ for single diffractive pp collisions at $\sqrt{s} = 7$ TeV as calculated using QGSJET-II-4 (red solid) and SIBYLL (green dashed). Partial contributions to $f_{\rm SD}(\xi)$ from low and high mass diffraction in QGSJET-II-4 are shown as black doted and blue dash-dotted lines respectively; yellow solid and black dashed lines are used for contributions of high mass diffraction at $b < 1.3$ fm and $b > 1.3$ fm.

may be found in Refs. [11, 19, 21, 26].

In Table 1 we compile the predictions of the above-discussed models for $\sigma_{pp}^{\rm inel}$ at $\sqrt{s} = 7$ TeV as well as the respective partial cross sections for non-diffractive $\sigma_{\rm ND}$, single high mass diffractive $\sigma_{\rm SD}^{\rm HM}$ (combined with double diffractive cross section $\sigma_{\rm DD}^{\rm LHM}$ corresponding to a high mass diffraction of one proton and a low mass excitation of the other one), double high mass diffractive $\sigma_{\rm DD}^{\rm HM}$, and single $\sigma_{\rm SD}^{\rm LM}$ and double $\sigma_{\rm DD}^{\rm LM}$ low mass diffractive collisions.[3] For comparison we add also the corresponding PYTHIA results taken from Ref. [4]. The considered subclasses of inelastic collisions differ in their efficiencies to generate a signal in scintillation detectors used in minimum-bias trigger selections (MBTS) of various LHC experiments. In non-diffractive events, all the kinematically accessible rapidity interval is covered by secondaries, hence, the probability to have a charged hadron inside a detector should approach 100% in that case.[4] In turn, high mass diffractive collisions contain large rapidity gaps not covered by secondary particles. Hence, a noticeable part of such collisions will be missed by the MBTS detectors - when the respective rapidity coverage of the detectors is fully inside the rapidity gaps. Finally, low mass diffractive interactions produce narrow bunches of secondaries in forward and/or backward hemisphere, such that almost the whole rapidity range, except its edges, is free of secondaries. Such events are likely to be missed by the triggers,[5] which was in particular the reason for combining $\sigma_{\rm SD}^{\rm HM}$ and $\sigma_{\rm DD}^{\rm LHM}$ together.

Importantly, the considered models differ not only in the predicted diffraction cross sections but also concerning mass distributions of diffractive states. This is illustrated in Fig. 2, where the distribution for $\xi = M_X^2/s$, $f_{\rm SD}(\xi) \equiv$

[3] In Table 1 we use *theoretical* definitions for low and high mass diffraction cross sections, which do not depend on an experimental trigger. For comparison, in [11] the diffractive event classification of the CDF experiment was applied to compare with the corresponding data.

[4] In QGSJET-II, there is a small (sub-mb) contribution of central diffraction (double Pomeron exchange) which we did not subtract from $\sigma_{\rm ND}$.

[5] In the QGSJET-II model, the low mass diffraction cross sections calculated in the multi-channel approach are assumed to correspond to diffractive final states described by the Pomeron-Pomeron-Reggeon ($\mathbb{PPR}$) asymptotics, with an approximate dM_X^2/M_X^3 diffractive mass distribution. Hence, one obtains some weak sensitivity of the MBTS detectors to the tail of the M_X distribution, as demonstrated in the following. Alternatively, one may assume that these cross sections correspond to a number of discrete low mass resonance states [13], in which case such events would be missed completely by the triggers.

	$\sigma_{\rm inel}$	$\sigma_{\rm ND}$	$\sigma_{\rm SD}^{\rm HM}+\sigma_{\rm DD}^{\rm LHM}$	$\sigma_{\rm DD}^{\rm HM}$	$\sigma_{\rm SD}^{\rm LM}+\sigma_{\rm DD}^{\rm LM}$
QGSJET II-04	69.7	49.6	5.7	7.3	7.1
QGSJET II-03	77.5	57.4	11.4	5.4	3.3
SIBYLL	79.6	65.7	12.2	1.7	0
PYTHIA	71.5	48.5	13.7	9.3	0

Table **1**: Model predictions for $\sigma_{pp}^{\rm inel}$ and for partial inelastic proton-proton cross sections (in mb) at $\sqrt{s} = 7$ TeV.

$\frac{\xi}{\sigma_{\rm SD}}\frac{d\sigma_{\rm SD}}{d\xi}$, is plotted for single diffractive pp collisions at $\sqrt{s} = 7$ TeV, as calculated using QGSJET-II-04 and SIBYLL. In contrast to the flat ξ-distribution of the SIBYLL model, which corresponds to the assumed dM_X^2/M_X^2 distribution for diffractive masses, a more complicated functional shape is predicted by QGSJET-II-04. The most striking difference is the sharp peak at $\xi \sim$ few GeV$^2/s$ corresponding to the production of low mass diffractive states. Additionally, the distribution for high mass diffraction changes from the $1/M_X^2$ behavior at very large M_X^2 to a steeper decreasing function at smaller M_X^2, which reflects the impact parameter b dependence of absorptive corrections to diffractive scattering. As noted in [10], strong absorptive corrections at small b result in the approximate $f(M_X^2) \sim 1/M_X^2$ distribution for diffractive masses. On the other hand, in very peripheral collisions absorptive corrections become weak and high mass diffraction is governed by the triple-Pomeron contribution with $f(M_X^2) \sim (M_X^2)^{-\alpha_{\mathbb{P}}}$ (in QGSJET-II-04 the soft Pomeron intercept $\alpha_{\mathbb{P}} = 1.16$ [11]). As a cross-check, one may compare two sub-samples of the simulated high mass diffraction collisions, with approximately equal event numbers: more peripheral collisions with $b > 1.3$ fm and more central ones ($b < 1.3$ fm). As one can see in Fig. 2, the latter case leads indeed to a flatter distribution for the diffractive mass.

Similarly, there are large differences between QGSJET-II and SIBYLL in the treatment of double high mass diffraction. As demonstrated in [10], already at the lowest order with respect to the triple-Pomeron coupling the corresponding picture is considerably more complicated than usually assumed in literature. Double diffractive final states may result from a collision which contains a single inelastic rescattering process characterized by the desirable structure of the final state (central rapidity gap) or from a collision with two inelastic rescatterings: one corresponding to single high mass diffraction of the projectile and the other - of the target, and with the corresponding rapidity gaps overlapping in the central region. Moreover, there exists a non-trivial interference between the two contributions [10].

3 Results for minimum-bias cross sections

The models discussed in the previous section have been used to generate hadronic final states corresponding to non-diffractive and various diffractive proton-proton collisions and to investigate selection efficiencies ε of the corresponding final states by minimum-bias triggers of the ATLAS experiment. Here we restrict ourselves with the MBTS_AND and MBTS_OR triggers which require at least one charged particle detected respectively at both positive ($\eta_1 < \eta < \eta_2$) and negative ($-\eta_2 < \eta < -\eta_1$) pseudorapidity intervals or in either of the two η-ranges, with $\eta_1 = 2.09$ and $\eta_2 = 3.84$ [4]. In addition, we consider the ChPart trigger selection which combines the MBTS_OR condition with the requirement of at least one charged hadron of transverse momentum $p_t > 0.5$ GeV being detected in the $|\eta| < 0.8$ range. When estimating the corresponding selection efficiencies we assume 100% detection probability for charged hadrons in the respective pseudorapidity intervals, thus neglecting potential loss of events due to less than 100% particle tracking efficiency. Though more accurate treatment, with the tracking efficiency properly taken into account, may result in somewhat lower trigger rates for inelastic processes, we do not expect the difference to be large because of the relatively

wide pseudorapidity intervals involved and high particle densities produced.[6]

The obtained model results for selection efficiencies of various inelastic processes, compiled in Table 2, confirm qualitative expectations of Section 2, demonstrating in particular that the ATLAS trigger selections have high efficiency for triggering non-diffractive interactions while being almost blind to low mass diffraction. On the other hand, we observe large differences between QGSJET-II and SIBYLL for $\varepsilon_{\rm DD}^{\rm HM}$, which is related to the treatment of double high mass diffraction in the two models. The contribution to $\sigma_{\rm DD}^{\rm HM}$ from the superposition of two simultaneous (projectile and target) single diffraction processes results in much narrower rapidity gap sizes (hence, in a smaller probability to miss the trigger) compared to the case of simple dM_X^2/M_X^2 distributions for the two diffractive masses, used in SIBYLL. It is noteworthy that $\varepsilon_{\rm DD}^{\rm HM}$ in QGSJET-II-03 is higher than in QGSJET-II-04 because Pomeron loops are neglected in the former model, hence, the above-discussed mechanism is the only one relevant for double high mass diffraction in that case. As anticipated in [2], the MBTS_AND and MBTS_OR triggers differ significantly in their sensitivity to single high mass diffraction: the ratio of the corresponding values for $\varepsilon_{\rm SD}^{\rm HM}$ is related to the ratio of the numbers of events with $\xi > \ln s/2 + \eta_1$ and $\xi > \ln s/2 - \eta_2$. This explains also the larger difference between the respective values of $\varepsilon_{\rm SD}^{\rm HM}$ for the two triggers in case of QGSJET-II-04 compared to SIBYLL - as in the former model single high mass diffractive events have a smaller probability to fall in the interval $\xi > \ln s/2 + \eta_1$ (c.f. blue dot-dashed and green dashed lines in Fig. 2). However, the values of $\varepsilon_{\rm SD}^{\rm HM}$ for QGSJET-II-03 appear to be similar to the ones for SIBYLL, which indicates that other effects, e.g. the rapidity density of produced hadrons, impact the results.

In Table 3, we compare the model predictions for "visible" cross sections for the various combinations of ATLAS minimum-bias triggers with experimental results; the corresponding values for PYTHIA from Ref. [4] are also added. It is easy to see that model extrapolations based on the CDF measurement of $\sigma_{pp}^{\rm tot}$ at the Tevatron are disfavored by the ATLAS results. Indeed, of the three models considered only QGSJET-II-04 agrees with the data within the uncertainties related to the luminosity determination. QGSJET-II-03 and SIBYLL exceed the measured MBTS rates by about 2σ and 3σ respectively while even stronger disagreement is observed for the ChPart event selection. On the other hand, the experimental results demonstrate the potential for discriminating between various theoretical models for soft multi-particle production. As an example, one may consider the approach of Refs. [12, 13], which predicts a much slower energy rise of the total and inelastic proton-proton cross sections and a significantly higher $\sigma_{\rm SD}^{\rm HM}$ compared to the one of Refs. [10, 27], realized in QGSJET-II-04. The mentioned differences are mostly due to specific assumptions on Pomeron-Pomeron interaction vertices, made in [12, 13], such that the scheme approaches the so-called "critical" Pomeron description in the "dense" limit of high energies and small impact parameters, as discussed in more detail in [10, 14]. In turn, this results in much smaller visible cross sections for the ATLAS minimum-bias triggers [2], which appear to be some 10 mb below the measured values.

One may doubt if the results of Ref. [2] may be modified by hadronization effects which have not been included in the corresponding analysis. We check such a possibility with QGSJET-II-04 by comparing the MBTS efficiencies for single and double high mass diffractive events obtained in two ways: based on charged particle tracking (as summarized in Table 2) or using the *theoretical* rapidity gap structure of individual events. In the latter case, we assume that an event is triggered if the rapidity coverage of the respective detectors is at least partly spanned by a cut Pomeron (which corresponds to an elementary "piece" of particle production in the model) produced when modeling the configuration of the interaction [11]. Alternatively, an event is not triggered if the detectors appear to be fully inside the *theoretical* rapidity gaps (defined by the cut Pomeron structure of the event). As is easy to see from Table 4, the corresponding theoretical efficiencies for the MBTS_OR selection coincide with the full MC results (Table 2) within few percents thereby confirming that the results of Ref. [2] are indeed disfavored by the data. On the other hand, the selection efficiencies for

[6] The possible exception is the ChPart selection which, however, has been corrected for the particle tracking efficiency of the ATLAS experiment in Ref. [4].

	QGSJET-II-04				QGSJET-II-03				SIBYLL		
	$\varepsilon_{\rm ND}$	$\varepsilon_{\rm SD}^{\rm HM}$	$\varepsilon_{\rm DD}^{\rm HM}$	$\varepsilon_{\rm LMD}$	$\varepsilon_{\rm ND}$	$\varepsilon_{\rm SD}^{\rm HM}$	$\varepsilon_{\rm DD}^{\rm HM}$	$\varepsilon_{\rm LMD}$	$\varepsilon_{\rm ND}$	$\varepsilon_{\rm SD}^{\rm HM}$	$\varepsilon_{\rm DD}^{\rm HM}$
MBTS_AND	95	25	76	0.3	95	29	82	0.2	98	28	59
MBTS_OR	100	64	96	7.1	100	63	97	6.4	100	62	86
ChPart	87	24	56	0.5	89	29	66	0.3	89	25	44

Table **2**: Model results for selection efficiencies (in %) of the ATLAS minimum-bias triggers to non-diffractive ($\varepsilon_{\rm ND}$), single high mass diffractive ($\varepsilon_{\rm SD}^{\rm HM}$), double high mass diffractive ($\varepsilon_{\rm DD}^{\rm HM}$), and low mass diffractive ($\varepsilon_{\rm LMD}$) proton-proton collisions at $\sqrt{s} = 7$ TeV.

	QGSJET-II-04	QGSJET-II-03	SIBYLL	PYTHIA	Exp. [4]
MBTS_AND	54.1	62.3	68.4	58.4	51.9±0.2
MBTS_OR	60.8	69.8	74.7	66.6	58.7±0.2
ChPart	48.4	57.7	62.3	45.7	42.7±0.2

Table **3**: Model predictions for visible cross sections (in mb) in the ATLAS minimum-bias detectors compared to the measured values [4] (the correlated 11% uncertainty of the experimental results related to the luminosity determination is not included in the quoted experimental errors).

	$\varepsilon_{\rm ND}$	$\varepsilon_{\rm SD}^{\rm HM}$	$\varepsilon_{\rm DD}^{\rm HM}$	$\varepsilon_{\rm LMD}$	$\sigma_{\rm obs}$
MBTS_AND	100	20	54	0	54.9 mb
MBTS_OR	100	66	91	0	60.3 mb

Table **4**: Selection efficiencies (in %) of various partial inelastic pp cross sections at $\sqrt{s} = 7$ TeV by the ATLAS minimum-bias triggers and the resulting visible cross sections, as obtained from the theoretical rapidity gap structure of final states in QGSJET-II-04.

the MBTS_AND trigger appear to be strongly modified by hadronization effects, which indicates that the latter change noticeably the rapidity gap structure of individual events. Hence, a complete MC treatment is a necessary prerequisite for inferring the high mass diffraction rate from a set of minimum-bias cross sections.

Clearly, without a good handle on the low mass diffraction, a determination of $\sigma_{pp}^{\rm inel}$ on the basis of measured minimum-bias cross sections will be strongly model-dependent. On the other hand, one may be tempted to use the ATLAS results to derive luminosity-independent estimations of the relative contributions of single and double high mass diffraction, $(\sigma_{\rm SD}^{\rm HM} + \sigma_{\rm DD}^{\rm LHM})/\sigma_{\rm abs}^{\rm HM}$, $\sigma_{\rm DD}^{\rm HM}/\sigma_{\rm abs}^{\rm HM}$, with $\sigma_{\rm abs}^{\rm HM} \equiv \sigma_{\rm inel} - \sigma_{\rm SD}^{\rm LM} - \sigma_{\rm DD}^{\rm LM}$. Such an information would be extremely valuable since model predictions for $\sigma_{\rm SD}^{\rm HM}$ and $\sigma_{\rm DD}^{\rm HM}$ are vastly different, as demonstrated in Table 1. However, the corresponding equation system for the ATLAS trigger selections

$$
\begin{aligned}
\sigma_{\rm MBTS-AND} &= \varepsilon_{\rm ND}^{\rm AND}\sigma_{ND} + \varepsilon_{\rm SD(HM)}^{\rm AND}(\sigma_{\rm SD}^{\rm HM} \\
&\quad +\sigma_{\rm DD}^{\rm LHM}) + \varepsilon_{\rm DD(HM)}^{\rm AND}\sigma_{\rm DD}^{\rm HM} \\
\sigma_{\rm MBTS-OR} &= \varepsilon_{\rm ND}^{\rm OR}\sigma_{ND} + \varepsilon_{\rm SD(HM)}^{\rm OR}(\sigma_{\rm SD}^{\rm HM} \\
&\quad +\sigma_{\rm DD}^{\rm LHM}) + \varepsilon_{\rm DD(HM)}^{\rm OR}\sigma_{\rm DD}^{\rm HM} \\
\sigma_{\rm ChPart} &= \varepsilon_{\rm ND}^{\rm ChPart}\sigma_{ND} + \varepsilon_{\rm SD(HM)}^{\rm ChPart}(\sigma_{\rm SD}^{\rm HM} \\
&\quad +\sigma_{\rm DD}^{\rm LHM}) + \varepsilon_{\rm DD(HM)}^{\rm ChPart}\sigma_{\rm DD}^{\rm HM}
\end{aligned}
$$

is ill-defined, mainly because of the strong correlation between the ChPart and MBTS triggers and due to the strong model-dependence of the selection efficiency for double high mass diffraction. Alternatively, one may combine non-diffractive and double high mass diffractive events together and restrict oneself with the MBTS results only. Applying a MC procedure to determine the selection efficiency for non-single-diffractive events ($\sigma_{NSD} \equiv \sigma_{ND} + \sigma_{DD}^{\rm HM}$), we obtain using QGSJET-II-04, QGSJET-II-03, and SIBYLL the results listed in Table 5. The corresponding values of $(\sigma_{\rm SD}^{\rm HM} + \sigma_{\rm DD}^{\rm LHM})/\sigma_{\rm abs}^{\rm HM}$ and of partial cross sections are compiled in Table 6. It is easy to see that the obtained relative rate of single high mass diffraction is strongly model-dependent. Hence, a direct measurement of high mass diffraction is required to discriminate between the various model approaches.

	QGSJET-II-04	QGSJET-II-03	SIBYLL
MBTS_AND	92	94	97
MBTS_OR	99	100	100

Table **5**: Model results for the selection efficiency $\varepsilon_{\rm NSD}$ (in %) of non-single diffractive events by the ATLAS minimum-bias triggers.

	QGSJET-II-04	QGSJET-II-03	SIBYLL
$\frac{\sigma_{\rm SD}^{\rm HM}+\sigma_{\rm DD}^{\rm LHM}}{\sigma_{\rm abs}^{\rm HM}}$	0.12	0.19	0.24
$\sigma_{\rm SD}^{\rm HM}+\sigma_{\rm DD}^{\rm LHM}$	7.4 mb	12 mb	16 mb
$\sigma_{\rm NSD}$	54 mb	51 mb	49 mb
$\sigma_{\rm abs}^{\rm HM}$	62 mb	63 mb	65 mb

Table **6**: Model-based estimations of the relative fraction of single high mass diffraction and of partial inelastic cross sections.

4 Outlook

In this work, we analyzed the model-dependence of the relation between the inelastic and various minimum-bias proton-proton cross sections, concentrating on the trigger selections of the ATLAS experiment and comparing the measured visible cross sections at $\sqrt{s} = 7$ TeV to predictions of a number of hadronic Monte Carlo generators used in the cosmic ray field. We demonstrated that the ATLAS results provide serious constraints on hadronic interaction models and allow one to discriminate between certain theoretical approaches to the treatment of soft multi-particle production. In particular, the minimum-bias trigger rates reported by ATLAS disfavor model extrapolations based on the CDF measurement of $\sigma_{pp}^{\rm tot}$ at the Tevatron. This will have an important impact on the studies of the nuclear composition of ultra-high energy cosmic rays with fluorescence light detectors [28, 29].

On the other hand, the strong model-dependence of the sensitivity of the ATLAS minimum-bias triggers to diffractive events, mainly due to the differences in the predicted diffractive mass distributions, prevents one from deducing the high mass diffraction rate from the measured visible cross sections. Moreover, the MBTS detectors prove to be insensitive to the contribution of low mass diffraction in proton-proton collisions. Hence, a reliable determination of the total inelastic pp cross section does not seem feasible without forward proton tracking by a dedicated experiment, like TOTEM [30].

Note added.

After this paper was submitted to the journal, a measurement of the inelastic proton-proton cross section for $\xi > 5 \times 10^{-6}$ has been reported by the ATLAS Collaboration [31]. Extrapolation of the result to the full kinematic range was found to be strongly model-dependent, primarily, due to strong sensitivity to model predictions for the diffractive mass distribution – which was also the main source of model-dependence discussed in this work.

Acknowledgments

The author acknowledges useful discussions with David d'Enterria and the support by the program Romforskning of Norsk Forskningsradet.

References

[1] R. Ulrich, R. Engel, and M. Unger, arXiv:1010.4310 [hep-ph]; R.D. Parsons, C. Bleve, S.S. Ostapchenko, and J. Knapp, arXiv:1102.4603 [astro-ph.HE].

[2] V.A. Khoze, A.D. Martin, and M.G. Ryskin, Phys. Lett. B **679**, 56 (2009).

[3] S. Navin, Proc. of the 40th Int. Symp. on Multiparticle Dynamics (ISMD-2010), University Press Antwerp 2011, pp. 233-238.

[4] G. Aad *et al.* (ATLAS Collaboration), Eur. Phys. J. C **71**, 1630 (2011).

[5] G.A. Schuler and T. Sjostrand, Phys. Rev. D **49**, 2257 (1994).

[6] V.N. Gribov, Sov. Phys. JETP **26**, 414 (1968).

[7] M.L. Good and W.D. Walker, Phys. Rev. **120**, 1857 (1960).

[8] A.B. Kaidalov, Phys. Rep. **50**, 157 (1979).

[9] O.V. Kancheli, JETP Lett. **18**, 274 (1973); J.L. Cardi, Nucl. Phys. B **75**, 413 (1974); A. Capella, J. Kaplan and J. Tran Thanh Van, *ibid.* **105**, 333

(1976); A.B. Kaidalov, L.A. Ponomarev and K.A. Ter-Martirosyan, Sov. J. Nucl. Phys. **44**, 468 (1986).

[10] S. Ostapchenko, Phys. Rev. D **81**, 114028 (2010).

[11] S. Ostapchenko, Phys. Rev. D **83**, 014018 (2011).

[12] M.G. Ryskin, A.D. Martin, and V.A. Khoze, Eur. Phys. J. C **54**, 199 (2008); *ibid.* **60**, 249 (2009).

[13] M.G. Ryskin, A.D. Martin, and V.A. Khoze, Eur. Phys. J. C **60**, 265 (2009).

[14] V.A. Khoze, A.D. Martin, and M.G. Ryskin, arXiv:1102.2844 [hep-ph].

[15] E. Gotsman, E. Levin, U. Maor, and J.S. Miller, Eur. Phys. J. C **57**, 689 (2008); E. Gotsman, A. Kormilitzin, E. Levin, and U. Maor, Nucl. Phys. A **842**, 82 (2010).

[16] E. Gotsman, E. Levin, and U. Maor, Eur. Phys. J. C **71**, 1553 (2011); *ibid.* **71**, 1685 (2011).

[17] R.S. Kolevatov, K.G. Boreskov, and L.V. Bravina, arXiv:1105.3673 [hep-ph].

[18] R.S. Fletcher *et al.*, Phys. Rev. D **50**, 5710 (1994);

[19] E.-J. Ahn *et al.*, Phys. Rev. D **80**, 094003 (2009).

[20] T. Sjostrand, S. Mrenna, and P. Skands, JHEP **05**, 026 (2006).

[21] S. Ostapchenko, Nucl. Phys. Proc. Suppl. **151**, 143 (2006); AIP Conf. Proc. **928**, 118 (2007).

[22] S. Ostapchenko, Phys. Lett. B **636**, 40 (2006); Phys. Rev. D **74**, 014026 (2006).

[23] K. Nakamura *et al.* (Particle Data Group), J. Phys. G **37**, 075021 (2010).

[24] F. Abe *et al.* (CDF Collaboration), Phys. Rev. D **50**, 5550 (1994).

[25] N.A. Amos *et al.* (E710 Collaboration), Phys. Rev. Lett. **68**, 2433 (1992).

[26] D. d'Enterria *et al.*, arXiv:1101.5596 [astro-ph.HE].

[27] S. Ostapchenko, Phys. Rev. D **77**, 034009 (2008).

[28] J. Abraham *et al.* (Pierre Auger Collaboration), Phys. Rev. Lett. **104**, 091101 (2010).

[29] R.U. Abbasi *et al.* (HiRes Collaboration), Phys. Rev. Lett. **104**, 161101 (2010).

[30] G. Anelli *et al.* (TOTEM Collaboration), JINST **3**, S08007 (2008).

[31] G. Aad *et al.* (ATLAS Collaboration), arXiv:1104.0326 [hep-ex].